Optimization of Particle Size for Hydrolysis of Pine Wood Polysaccharides and its Impact on Milling Energy

Miguel Angel Zamudio-Jaramillo*, Agustín Jaime Castro-Montoya*‡ Rafael Maya Yescas*, María del Carmen Chávez Parga* Juan Carlos González Hernández** and Jaime Saucedo Luna*

*Facultad de Ingeniería Química, Universidad Michoacana de San Nicolás de Hidalgo, Morelia, Michoacán, México

**Depto. Ingeniería Química e Ingeniería Bioquímica, Instituto Tecnológico de Morelia, Morelia, Michoacán, México

(mikezamjara@hotmail.com, ajcastrofiq@gmail.com, rafaelmayayescas@yahoo.com.mx, carmen_pchavez@yahoo.com, jcgh1974@hotmail.com, saucedol@hotmail.com)

‡ Corresponding Author; Agustín Jaime Castro-Montoya, Francisco J. Múgica s/n Col. Félix Ireta, 58030, Morelia, Michoacán, México, Tel: 01(443) 3223500 ext. 1207, ajcastrofiq@gmail.com

Received: 03.03.2014 Accepted: 22.05.2014

Abstract- Wood milling is an intensively energy consuming operation that has a significant effect on energy yield of ethanol production processes as particle size is an important factor in productivity of saccharification methods. Fiber particle size was optimized for a very wide range of treatment conditions (temperature, agitation, and solid loads) for acid hydrolysis in a batch reactor. Also, heat and mass transfer effects were analysed by calculating the Thiele and Prater modulus at experimental conditions. Multivariate optimization results show that using a length-weighted fiber mean diameter (D_{L21}) of 1.21-2.68 mm, a better sugar yield, concentration and lower furan production can be achieved. Agitation allowed a simultaneous particle size reduction and hydrolysis of polysaccharides. Heat and mass transfer studies suggest that acid diffusion is only important for hemicellulose hydrolysis at very high temperature and that particles are nearly isothermal. These results show that about 30% of the required energy for milling can be saved by using optimal particle size.

Keywords- Wood, ethanol, acid hydrolysis, saccharification.

1. Introduction

Bioethanol from lignocellulosic biomass is one of the most promising technologies for fuel production because of the abundance of lignocellulosic biomass [1, 2], its very low net greenhouse gases emissions and its renewability [1, 3, 4]. To produce ethanol from lignocellulose biomass it is necessary to hydrolize its structural polysaccharides (cellulose and hemicellulose) to monomer sugars (mainly glucose and xylose) so they can be fermented by microorganisms. Although there are several methods of hydrolysis including acid, enzymatic, steam explosion and microwave treatments, acid hydrolysis is one of the most frequently used method due to its technological readiness [2,5]. In this process lignocellulosic biomass is treated with an acid solution to break the glycosidic bond in the cellulose and hemicellulose chemical structure by the addition of a water molecule. In this reaction a proton from the acid solution catalyses the hydrolysis of the glycosidic bonds. As hydrolysis takes place, monomeric sugars also are converted to degradation products like furans, i.e. furfural and hydroxymethylfurfural (HMF), which are inhibitors for the subsequent fermentation process [6, 7]. Hydrolysis of cellulose and hemicellulose from biomass is a heterogeneous, solid-liquid reaction. Some studies in continuous reactors report a flow rate-dependent reaction rate [8,9], negative effects over sugar yield at high solid loads [10]; deviations from Arrhenius model predictions on temperature changes [11] and effects of cellulose crystalline index in hydrolysis reaction rate [12,13]. However studies in this area are limited. Particle size in wood hydrolysis is important for both, reaction rate and yield to monomeric sugar, and also for

energy balances. Typical particle sizes for thermochemical hydrolysis are the retained fraction in 40-60 mesh or about 0.42-0.25 mm [8, 12, 14]. Size reduction is an energy intensive operation that has been largely missed in energetic balances [15, 16]. Estimations of energy consumption for biomass comminution are about 300-600 wh/kg to obtain a particle size of 2 mm. In the case of wood this represents about 10-30% of the energy that can be obtained from biomass as ethanol [16]; this energy consumption compromises the energetic sustainability of the process. Particle size also have implications on suspension rheology. Lignocellulosic biomass fiber suspensions behave as a Bingham plastic with an increasing viscosity at higher solid loads. This has an important impact in external flow pattern around the particle, clump formation and agitation power consumption [17, 18]. Since phenomena like heat and mass transport are influenced by both, particle size and flow pattern, the objective of this work was to assess the effect of particle size on concentration and yield to glucose during the wood hydrolysis process, and to study the role of mass and heat transfer on them.

2. Materials and Methods

2.1. Biomass and Particle Characterization

Pine wood sticks were obtained from a wood sawmill located near Morelia, Mexico; this material was milled using a knife mill. The resulting fibers were classified by size using a standard sieve vibrator for 30 min, using 10, 20, 40, 60, 120 mesh sieves. In order to avoid oxidation, the fractions were stored in sealed plastic bags and air was extracted using a vacuum pump. For particle size measurements, photographic images were taken of the fibers from all sieve fractions using an optical microscope (Steren) in a dark contrast background. Data for maximum and minimum Feret diameter in the pictures were obtained using the ImageJ software (NIH Image,http://rsbweb.nih.gov/ij/; [19]) as measurements of fiber length (*L*) and diameter (*d*) respectively. At least 500 particles per sample were measured, with the following restrictions: a) only complete particles were measured. b) Particle data with a solidness factor lower than 0.7 were discarded as were interpreted as overlapped fibers. Data for diameter and length were used to calculate the length weighted fiber mean diameter (D_{L21}) using equation (1):

$$D_{L21} = \frac{\sum_i n_i L_i d_i^2}{\sum_i n_i L_i d_i} \approx \frac{4}{S_f^v} \quad (1)$$

For wood chemical characterization the Technical Association of the Pulp and Paper Industry (TAPPI) and American National Standards Institute (ANSI) methods were used. Tests for humidity and extractible substances (TAPPI T-264), Lignin (TAPPI T-222), cellulose (ANSI/ASTM 1977b) and hemicellulose (ANSI/ASTM 1977b) were performed.

2.2. Reactor and Hydrolysis Experiment

Hydrolysis experiments were performed in a SS304 reactor equipped with a thermowell and a K-thermocouple with a measurement range of 10°C-400°C and a P.I.D. controller. Temperature was controlled using a heating plate (Isotemp) and agitation was provided using a one inch magnetic bar. For hydrolysis experiments Liquid/Solid ratio (mL liquid/g solid biomass) was modified by loading different amounts of biomass into the reactor and 15 mL of 0.4% (w/w) H_2SO_4 solution was added. Such concentration was determined in previous work [20]. The reactor was sealed using Teflon ribbon and was preheated in an oil bath at 250°C. When target temperature of the experiment was reached, the reactor was introduced into another oil bath at target temperature and agitation was activated if needed in the respective treatment. When reaction time was achieved, the reactor was cooled into running cold water. Using this procedure heating time was about 3-5 minutes and cooling time was about 30 s. Reactor content was recovered and was vacuum filtered using filter paper and a Buchner funnel. Liquid phase from filtration procedure was frozen and stored for chemical analysis and the material retained in the filter was washed thoroughly using distilled water to remove remaining acid and dried at 65°C overnight. Remaining solids weight was determined by gravimetric method.

A reduced face centered central composite design was used for the experiments Liquid/solid ratio (L/S) (10-20), stirring speed (0-1200) rpm, temperature (140-210)°C and particle size (60-20 mesh sieve retained fractions or 0.84-0.25 mm sieve size) were factors in the experimental design resulting in 18 treatments (Table 1). For each treatment replicate runs were performed at 0, 5, 20, 40 minutes.

Table 1. Experimental design for hydrolysis experiments.

	L/S	T (^oC)	Ag (rpm)	Mesh no fraction*
T1	10	140	1200	20
T2	15	175	600	60
T3	20	140	0	60
T4	15	210	600	40
T5	10	175	600	40
T6	20	140	1200	60
T7	15	175	600	20
T8	15	175	0	40
T9	20	210	0	20
T10	15	175	1200	40
T11	10	140	0	20
T12	10	210	0	60
T13	15	140	600	40
T14	20	210	1200	20
T15	20	175	600	40
T16	15	175	600	40
T17	10	210	1200	60
T18	15	175	600	40

* Opening sieve size: 20 mesh = 0.84 mm, 40 mesh =0.42 mm, 60 mesh = 0.17 mm.

2.3. Chemical Analysis

Glucose and xylose concentrations from the liquid phase from the filtered hydrolysates were measured using HPLC with a Metacarb (Varian) column heated at 70°C with a column oven. Deionized water was used as a mobile phase with a flow rate of 1 mL/min for 15 min. Detection was performed with a IR detector (Varian). Glucose and xylose yield were calculated from concentration data using mass balance, reaction stoichiometry and were corrected for humidity and extractive content obtained from wood analysis. Furan compounds were measured with the method reported by Martínez et al. [21]. Filtered hydrolysates were diluted with distilled water to a concentration of 0.5-1 mg/l and absorbance was read at 278 nm using a UV-spectrophotometer Jenway. Furan concentration was calculated with a standard curve prepared with 2-furfuraldehyde (Sigma).

2.4. Statistical Analysis and Numerical Optimization

Results from the experimental design were adjusted to a second order linear model shown in Eq. (2) to describe the effect of all factors by the Least Squares Method and the significance of the parameters was evaluated at α=0.05.

$$y_n = \beta_0 + \sum_{i=1}^{k}\beta_i x_i + \sum_{i=1}^{k}\beta_{ii} x_i^2 + \sum_{j}^{k}\sum_{i=1}^{k}\beta_{ik} x_i x_j + \varepsilon_i \quad (2)$$

Where $\hat{y}_n$ is any of the response variables (glucose, xylose and furan concentrations, and yield of glucose and xylose); x_i, and x_j are the k=5 factors (agitation rate, temperature, L/S ratio, particle size and time) and the β coefficients are regression parameters.

Multivariate optimization of the process was achieved using the desirability function approach [22]. This method consists in transforming a multivariate problem to an univariate one by defining an objective function where desirability D (a measure of "goodness" of the process) is to be optimized. D is calculated from individual desirabilities of all response variables (d) using Eq (3).

$$D = (d_1 \times d_2 \times \ldots \times d_n)^{1/k} \quad (3)$$

Where:

$$d_i = \begin{cases} 0 & \hat{y}_i \le y_{i*} \\ \left[\dfrac{\hat{y}_i - y_{i*}}{y_i^* - y_{i*}}\right]^r & y_{i*} \le \hat{y}_i \le y_i^* \\ 1 & \hat{y}_i \ge y_i^* \end{cases}$$

For response variables to be maximized (i.e. sugar concentrations and yields) and:

$$d_i = \begin{cases} 1 & \hat{y}_i \le y_{i*} \\ \left[\dfrac{\hat{y}_i - y_i^*}{y_{i*} - y_i^*}\right]^r & y_{i*} \le \hat{y}_i \le y_i^* \\ 0 & \hat{y}_i \ge y_i^* \end{cases}$$

For response variables to be minimized (furan concentration is to be minimized due to its toxicity to the further fermentation process).

y_{i*} and y_i^* are lower and upper limits for response variable y_i. Optimization of the effect of the reaction conditions on process desirability was performed by the Simplex algorithm using Software Statistica v8.0® (Statsoft). Since cellulose and hemicellulose have different reaction rates there can be conflictive objectives for glucose and xylose concentration. This also can happen between sugar yields and concentrations because with an L/S decrease (increase of solid load) sugar concentrations would increase and yields decrease. For this motive optimization was performed changing optimization parameters to obtain results for different process configurations (i.e. two stage processes).

2.5. Mass and Heat Transfer Analysis

In order to clarify mass and heat transfer role in the process, Thiele modulus ϕ and Prater number β were calculated at initial experimental reaction conditions using $\phi = \frac{R}{2}\sqrt{\frac{k}{D_{eff}}}$ and $\beta = \frac{D_{eff} C_b \Delta H}{K_T T_b}$ [23]. Were R is fiber radius (R= D_{L21}/2), C_b is bulk liquid molar acid concentration (7700 mol/m^3), ΔH is reaction enthalpy [3.8 kJ/mol; [24]], K_T is thermal effective conductivity of the solid phase and was calculated as K_T= Kw(1- ε)+(K_{H20*} ε) (K_w=0.14 W/mK; K_{H20}=0.54 W/mK, ε=0.87 [25]), and T_b is bulk liquid temperature. D_{eff} is the effective diffusivity of sulfuric acid in the lignocellulosic material, which was considered a temperature-dependent property and was calculated with the model proposed by Kim et al., [14]. For simplification, cellulose and hemicellulose hydrolysis were modeled as first order reactions and k is first order reaction constant following Arrhenius temperature dependency. Table 2 summarizes reaction models, parameters and references for calculation of rate constants and effective diffusivity at different reaction conditions.

Table 2. Resume of kinetic parameters and models used for Thiele modulus and Prater number calculations.

Effective diffusivity		Ref.
$D_{eff} = D_0 e^{-\frac{E}{RT}}$	D_0=6.08 x10^{-8} m^2/s, E=3500 cal/mol	[14]
Cellulose hydrolysis		.
$k = k_0[H]^m e^{-\frac{E_A}{RT}}$	E_A =42.9 kcal/mol, k_0=4.12E+18 s^{-1} m=1.21	[26]
$k = k_0 \%Ac^m e^{-\frac{E_A}{RT}}$	E_A =42.5 kcal/mol, k_0=2.15E+17 s-^{1}, m=1.16	[27]
$k = k_0 e^{-\frac{E_A}{RT}}$	E_A =33.2 kcal/mol $k_{0=}$1.81E+13 s^{-1}	[28]
Hemicellulose hydrolysis		
$k = k_0 e^{-\frac{E_A}{RT}}$	E_A =27.4 kcal/mol, k_0=8.82E+11s^{-1}	[29]
$k = k_0 \%Ac^m e^{-\frac{E_A}{RT}}$	E_A =26.7 kcal/mol, k_0=2.33E+12 s^{-1}, m=0.68	[30]
$k = k_0 \%Ac^m e^{-\frac{E_A}{RT}}$	E_A =30.9 kcal/mol, k_0=1.46E+15 s^{-1}, m=1	[31]

3. Results and discussion

3.1. Wood Analysis and Particle Classification

Table 3 shows the composition obtained for the pine wood samples. The main components were cellulose and hemicellulose, and significant amounts of extractives were also obtained. These results are approximate to the values reported by Sjöström [32]. These data were used to calculate maximum possible sugar concentration to calculate sugar yields.

Table 3. Results of composition analysis of wood samples.

	% weight
Humidity	6.6±0.1
Extractives	4.5±0.3
Lignin	20±1.1
Cellulose	35.5±0.6
Hemicellulose	22±0.1

Particle classification yielded the particle distribution shown in Table 4. D_{L21} is very similar to mean fiber diameter so fibers had a very narrow fiber length variability. It also can be seen that wood fibers were classified more according to diameter size than by length. However, heat and mass transfer are supposed to be unidirectional in a radial direction toward the fiber center so the particle classification was satisfactory.

3.2. Hydrolysis Results

Results of hydrolysis experiments in the batch reactor are shown in Figs. 1 and 2. In Figs. 1a and 1b, glucose, xylose and furan concentration are shown as the main reaction products in all treatments. However other compounds like cellobiose (0.1- 1.5 g/l) and arabinose (0.1-0.5 g/l) were detected. Also, it can be seen that xylose concentration rose faster than glucose. This is because hemicellulose hydrolysis to xylose monomers is faster than cellulose conversion to glucose. This means that glucose and xylose maximum concentrations are obtained at different times.

Table 4. Particle size characterization.

Mesh no fraction	Sieve Size mm	Mean particle diameter Mm	Mean particle lengthMm	D_{L21} mm
20	0.84	1.98 ± 0.04	5.30 ± 0.13	2.1
40	0.42	1.09 ± 0.03	3.01± 0.12	1.2
60	0.25	0.14 ± 0.06	0.38 ± 0.24	0.2

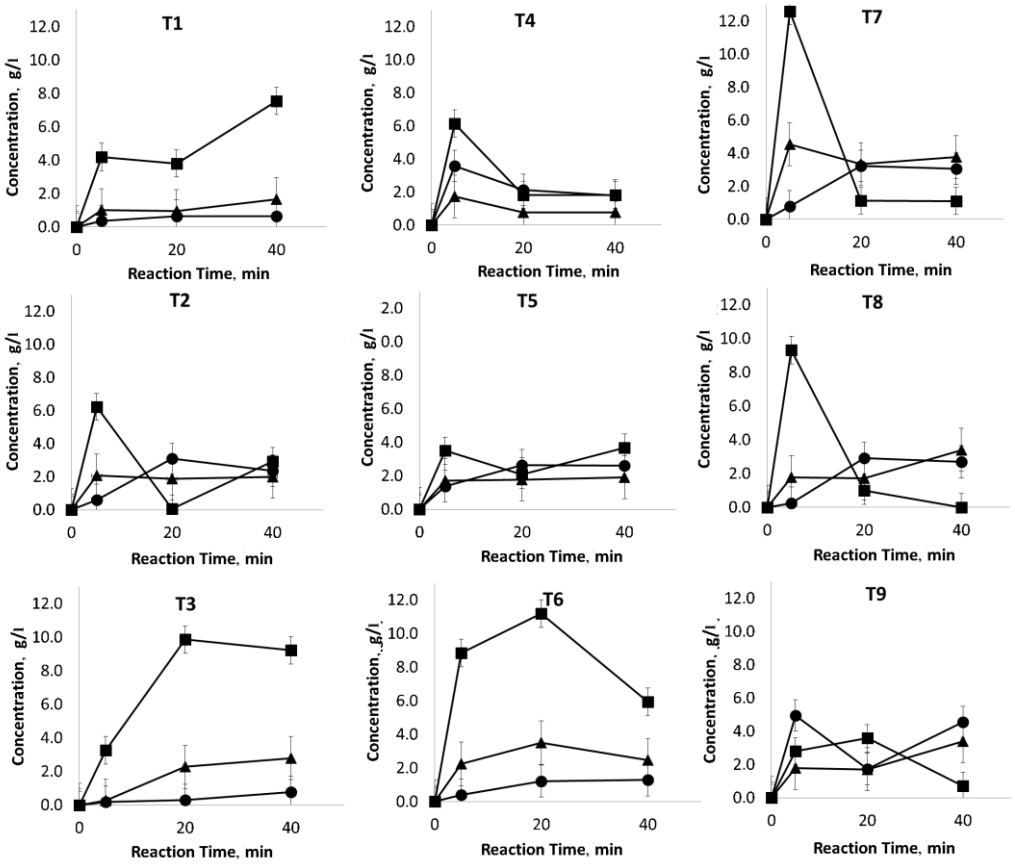

Fig. 1. a. Sugar and furans obtained in the batch reactor. Glucose (▲), xylose (■), Furans (●). See Table 1 for treatment conditions. Error bars represent 95% confidence interval calculated from replicated data.

Furan production can be seen in all treatments showing carbohydrate degradation. Total furans vary widely depending on experimental conditions in the treatments but for most treatments inhibition would occur if the resulting hydrolysates were fermented since inhibition for furan compounds in the fermentation process occurs above 1 g/l for furfural and 2 g/l for HMF [7,33]. It can be seen as well

that furan concentration also diminishes probably due to its conversion to other compounds like levulinic acid [34].

Figs 2a and 2b show that particle size is reduced as reaction takes place but this effect is sharper in large particle treatments. Agitation causes an even sharper reduction of fiber D_{L21} due to shear stress caused by magnetic bar achieving a simultaneous milling and saccharification process.

Figure 3 shows the changes during the hydrolysis process of a selected experiment in which a moderate agitation rate is used and a great particle size reduction is achieved as process took place. Zhu et al. [16] milled woody biomass pretreated with acid and reported a 80% saving of energy consumption. This results can be used to develop a simultaneous milling and saccharification process.

Statistical analysis from data in Figs. 1 and 2 are summarized in Table 5. As expected, temperature and time were the most influential factors for all response variables. Particle size had a significant effect in all responses with the exception of furan concentration. In sugar yields and concentration, particle size had a significant quadratic effect which means it can be optimized in a nearby region of the experimental runs performed. L/S ratio had a negative effect over sugar yields but showed little influence over sugar concentrations probably because a higher L/S enhances sugar degradation to furans, as can be seen in the significant effect of L/S on furan concentration. Agitation as an independent factor shows very weak impact over product conversion. However, as an interaction with L/S ratio it contributes to have a higher sugar concentration and a higher particle size reduction and solubilization of solids.

3.3. Optimization Results

Table 6 shows the optimal hydrolysis conditions yield by application of the simplex algorithm to the adjusted function in statistical analysis. For all cases a low temperature-high time had better results in all response variables since a more intense process yields sugar degradation to furans. The conditions for optimal glucose and xylose concentrations were very different. This means optimal conditions for high xylose concentration and yield results in low yield and concentrations of glucose so a two stage process is a better option as other authors have recommended [35]. It is remarkable that in optimization runs where a compromise between sugar concentration and yields is requested (E, F, G), optimal results lays in large particle and high solid loads regions, and in those cases agitation is needed. This can be interpreted as follows: Agitation contribution is to reduce particle size so higher particle size and higher solid loads can be used.

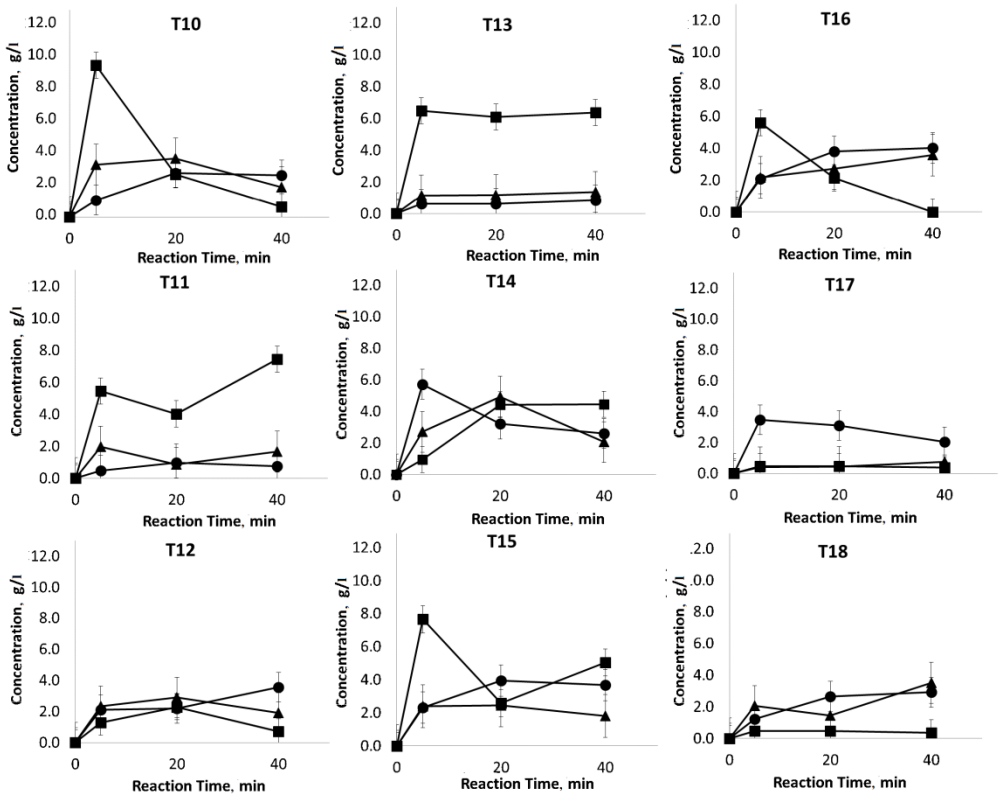

Fig. 1. b. Sugar and furans obtained in the batch reactor. Glucose (▲), xylose (▄), Furans (●). See Table 1 for treatment conditions. Error bars represent 95% confidence interval calculated from replicated data.

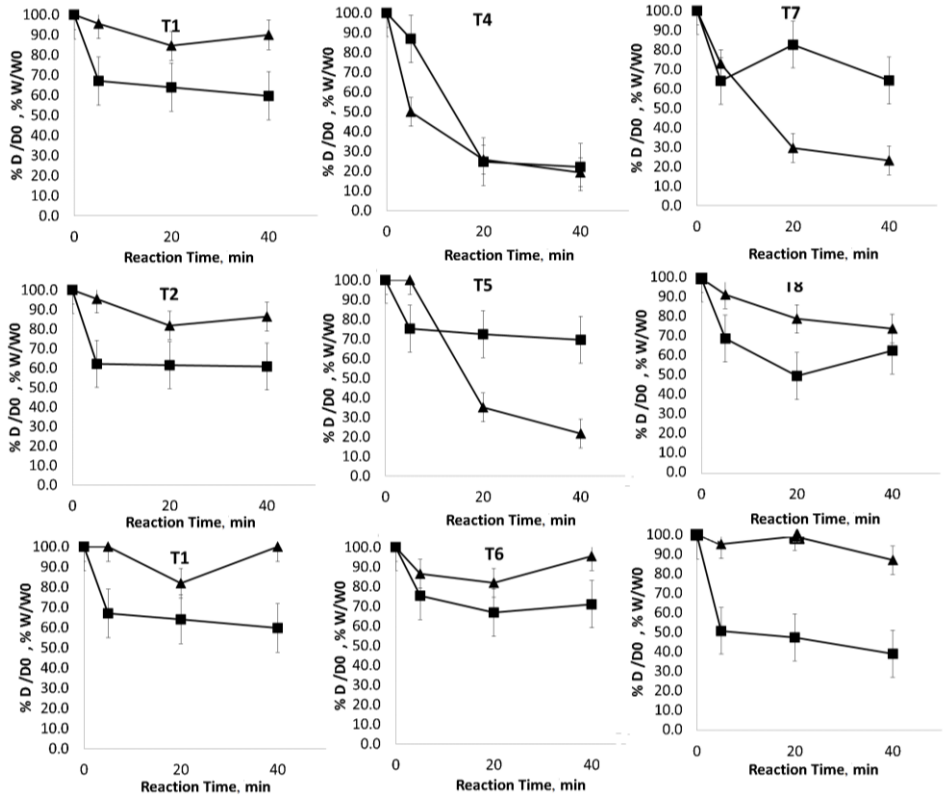

Fig. 2. a. Particle size and remaining solids weight reduction in the hydrolysis process. D/D_0 is ratio of fiber D_{L21} on initial fiber mean diameter (▲), W/W_0 is ratio of remaining solids on initial dry weight solids load (▄). See Table 1 for treatment conditions. Error bars represent 95% confidence interval calculated from replicated data.

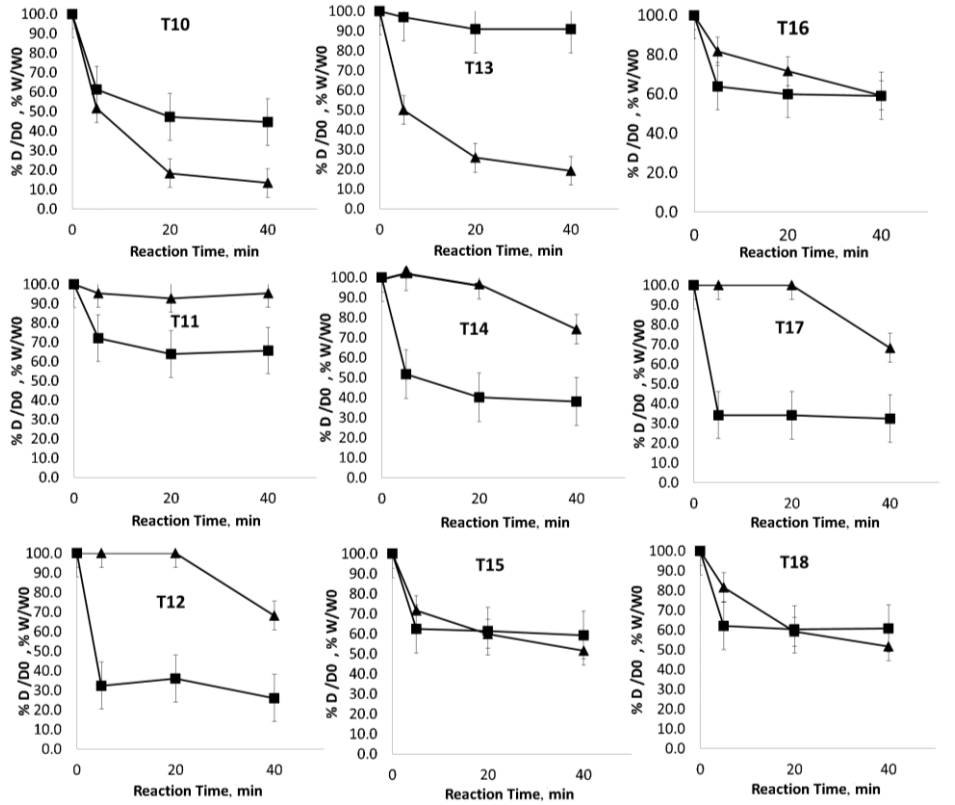

Fig. 2. b. Particle size and remaining solids weight reduction in the hydrolysis process. D/D_0 is ratio of fiber D_{L21} on initial fiber mean diameter (▲), W/W_0 is ratio of remaining solids on initial dry weight solids load (▄). See Table 1 for treatment conditions. Error bars represent 95% confidence interval calculated from replicated data.

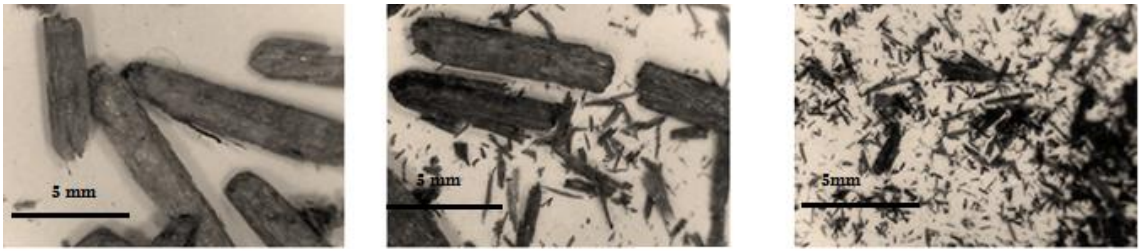

Fig. 3. Photographic images of treated wood fibers. Conditions: temp 175° C; L/S 15, 600 rpm, initial D_{L21}=2.1mm, H_2SO_4 0.4%. A) 5 min. B) 20 min. C) 40 min.

This is interesting since efforts of many works are aimed to increase solid loads so higher concentrations can be achieved without compromising yield since raw materials can be about 40% of the product costs [36]. Experimental runs were performed in the reactor to validate the model predictions and results are shown in Table 7. Although experimental data differ statistically from predicted response values they are somewhat approximate with a mean difference of 2.6 g/l and a standard error of 1.61 g/l, and generally better results were obtained from the experimental experiments run previously obtaining about 2 fold of the best treatments shown in Fig 1a and 1b. It can be seen that reduction of furan concentration to < 1 g/l was successful in most of the optimization trials so inhibition for furan compounds was avoided.

Table 5. Factor coefficients estimation and probability from the ANOVA of hydrolysis data*.

	Product concentration			Sugar Yield		D/D_0	W/W_0
	Gluc(g/l)	Xylose (g/l)	Furan (g/l)	Xylose Yield	Glucose Yield		
R^2	0.68	0.62	0.70	0.72	0.63	0.82	0.80
L/S	0.16	0.53	**0.42**	**-1.47**	**-8.35**	3.77	-3.96
L/S^2	-0.11	0.68	0.33	-0.63	2.82	0.36	-1.05
Temp	-0.08	**-1.83**	**0.72**	-0.30	**-10.18**	**-23.81**	**-19.21**
Temp^2	**-0.75**	0.21	**-0.54**	**-2.96**	1.15	3.69	0.46
Agitation	0.18	0.60	-0.04	0.71	3.36	**-22.90**	-3.16
Agitation^2	**0.36**	-0.36	-0.19	**1.44**	-1.98	-1.10	**-9.14**
D_{L21}	**0.71**	0.31	0.14	**2.86**	1.89	**-12.61**	3.08
D_{L21}^2	**-0.57**	**1.72**	0.12	**-2.25**	**9.56**	-1.66	1.56
Time	**0.92**	**1.64**	**1.15**	**3.60**	**9.02**	**-22.21**	**-21.78**
time^2	**-1.57**	**-4.60**	**-1.11**	**-5.59**	**-24.10**	**11.43**	**22.87**
L/S*Temp	**-0.85**	-0.99	0.15	**-4.01**	-2.73	**22.19**	-3.55
L/S*agitation	**0.07**	**-0.22**	0.17	-0.03	-1.95	**9.10**	2.24
Temp*agitation	0.04	0.47	-0.12	0.47	3.21	**-20.12**	0.76
L/S* D_{L21}	0.48	0.38	0.18	**2.15**	2.98	2.16	**8.73**
Temp* D_{L21}	0.07	-0.21	-0.10	-0.18	3.00	5.97	**8.70**
ag* D_{L21}	-0.17	-0.53	0.03	-0.80	-3.42	**-9.33**	-1.35
L/S*time	0.04	0.21	0.01	**-0.82**	-3.12	3.50	2.22
Temp*time	**-0.23**	**-1.48**	**0.36**	-0.62	**-8.26**	**-13.83**	**-8.49**
agitation*time	-0.02	0.12	-0.13	-0.14	1.06	**-9.01**	-2.52
D_{L21}*time	0.15	-0.12	0.11	0.34	-2.16	1.42	0.90

* Bold numbers represent a significant effect for the corresponding response variable. Coefficients are codified with factor levels ranging from 1 to -1 according with experimental design in Table 1. D/D_0 is the ratio of fiber diameter on initial fiber diameter. W/W_0 is the ratio of remaining solid dry weight on initial loaded dry weight wood.

Table 6. Numerical optimization results for wood hydrolysis.

	Optimization objective	Predicted Factor values at optimal conditions					Predicted Response values at optimal conditions				
		L/S	T (°C)	Ag (rpm)	D_{L21} (mm)	Time (min)	Concentration(g/l)			Sugar yield %*	
							Gluc	Xyl	Furans	Xyl	Gluc
A	max Glucose yield + min furan concentration	15	136	390	1.21	23.59	22.53	11.64	0.13	46.56	64.37
B	max Gluc concentration + min furan concentration	6.3	155	276	2.68	35.39	25.52	14.95	0.84	39.86	48.61
C	max Xylose yield + min furan concentration	12	121	240	2.68	23.59	16.03	26.00	2.83	85.97	37.86
D	max xylose concentration + min furan concentration	9.1	119	875	1.21	47.18	22.21	29.00	0.05	65.73	35.96
E	max gluc conc + max gluc yield+ min furan concentrations	5.8	142	180	2.68	35.39	67.20	14.95	0.84	19.93	64.00
F	max xyl conc+ min xyl yield+ min furan concentration	7.1	119	600	2.68	35.39	24.52	26.71	1.14	46.30	30.36
G	max all concentrations, yields + min furan concentration	9.3	125	550	2.68	23.59	31.10	27.00	1.14	61.20	50.36

*Sugar yield was calculated from maximum theoretical maximum.

Table 7. Experimental results at numerically optimized conditions*.

	Optimization objective	Response Experimental data at optimal conditions				
		Concentration (g/l)			Sugar Yield %	
		Gluc	Xyl	Furans	Xyl	Gluc
A	max Glucose yield + min furan concentration	17.34±1.1	16.10±0.5	0.17±0.13	64.40±1.1	69.36±0.5
B	max Gluc concentration + min furan concentration	19.12±3.5	11.20±1.2	0.14±0.12	29.87±3.5	50.99±1.2
C	max Xylose yield + min furan concentration	9.42±2.1	19.10±2.2	1.32±0.42	63.16±2.1	31.15±2.2
D	max xylose concentration + min furan concentration	25.78±2.1	35.10±2.6	0.04±0.23	79.56±2.1	58.43±2.6
E	max gluc conc + max gluc yield+ min furan concentrations	45.10±4.5	10.73±4.2	0.23±0.17	14.31±4.5	60.13±4.2
F	max xyl conc+ min xyl yield+ min furan concentration	15.26±0.5	25.20±3.1	0.91±0.21	43.68±0.5	26.45±3.1
G	max all concentrations, yields + min furan concentration	22.10±2.6	16.71±1.7	1.91±1.1	37.88±2.6	50.09±1.7

* See Table 6 for hydrolysis conditions, sugar yield was calculated from therotical maximum.

3.4. Heat and Mass Transfer Analysis

Thiele modulus for diffusion of sulfuric acid and Prater number results are shown in Table 8. It can be seen that φ in most cases is lower than 1.3 so acid transport to the particle center is not rate limiting. This is consistent with the calculations reported by Vidal [37] which showed similar results using dynamical simulations.

Table 8. Thiele modulus and Prater number for reaction conditions*.

Temp °C	D_{L21} mm	Deff m^2/s	Cellulose			Hemicellulose			Prater number	ΔT_{max} °C
			ϕ[26]	ϕ [27]	ϕ [28]	ϕ [29]	ϕ [30]	ϕ [31]		
140	1.2	8.56E-10	0.036	0.066	0.028	1.318	2.441	0.527	1.18E-04	0.05
175	0.2	1.19E-09	0.024	0.041	0.017	0.399	0.713	0.188	1.52E-04	0.07
140	0.2	8.56E-10	0.003	0.006	0.003	0.128	0.237	0.051	1.18E-04	0.05
210	1.2	1.59E-09	0.810	1.248	0.545	6.616	11.493	3.592	1.88E-04	0.09
175	1.2	1.19E-09	0.153	0.255	0.110	2.500	4.474	1.179	1.52E-04	0.07
140	0.2	8.56E-10	0.003	0.006	0.003	0.128	0.237	0.051	1.18E-04	0.05
175	2.1	1.19E-09	0.251	0.419	0.180	4.113	7.359	1.939	1.52E-04	0.07
175	1.2	1.19E-09	0.153	0.255	0.110	2.500	4.474	1.179	1.52E-04	0.07
210	2.1	1.59E-09	1.333	1.452	0.896	10.882	18.905	5.909	1.88E-04	0.09
175	1.2	1.19E-09	0.153	0.255	0.110	2.500	4.474	1.179	1.52E-04	0.07
140	2.1	8.56E-10	0.036	0.066	0.028	1.318	2.441	0.527	1.18E-04	0.05
210	0.2	1.59E-09	0.129	0.199	0.087	1.055	1.833	0.573	1.88E-04	0.09
140	1.2	8.56E-10	0.022	0.040	0.017	0.801	1.484	0.320	1.18E-04	0.05
210	2.1	1.59E-09	1.333	1.352	0.896	10.882	18.905	5.909	1.88E-04	0.09
175	1.2	1.19E-09	0.153	0.255	0.110	2.500	4.474	1.179	1.52E-04	0.07
175	1.2	1.19E-09	0.153	0.255	0.110	2.500	4.474	1.179	1.52E-04	0.07
210	0.2	1.59E-09	0.129	0.199	0.087	1.055	1.833	0.573	1.88E-04	0.09
175	1.2	1.19E-09	0.153	0.255	0.110	2.500	4.474	1.179	1.52E-04	0.07

*References indicate the source for the reaction kinetic parameters.

On the contrary, in the case of hemicellulose, only small particle/low temperature treatments satisfy φ < 1.3 showing a strong mass transfer limitation effect in large particle/high temperature treatments. To extend the results to other treatment conditions we delimited conditions for mass transfer limitations. Line plotted in Fig. 4a and 4b Shows a limit for mass transfer limited conditions (ϕ>1.3).This means that treatments under the line would not be restricted for intra-particle acid transfer to the fiber. Since hemicellulose has a faster hydrolysis rate, the mass transfer is more important and the non-restricted region is narrower. Nevertheless most processes for xylan hydrolysis are performed at low temperatures (110-140°C).

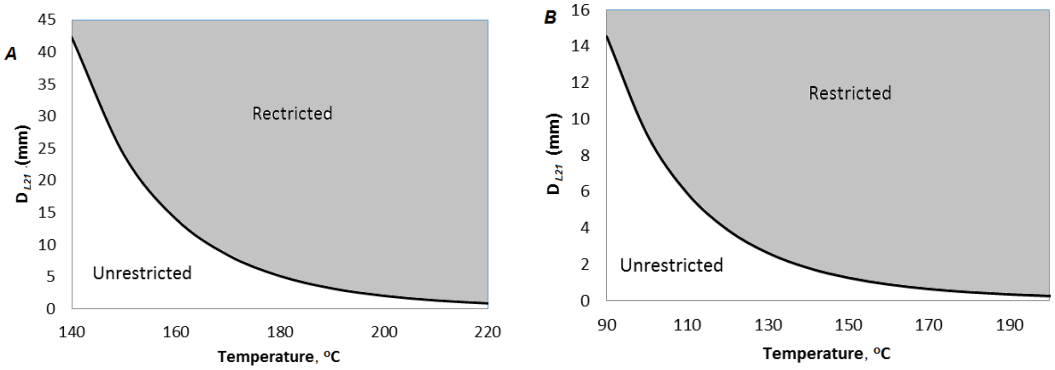

Fig. 4. Diffusion restricted regions for pine wood hydrolysis A) Cellulose B) Hemicellulose. Models, kinetic parameters and references are summarized in Table 3. Lines represent ϕ=1.3 treatments for mean of data results.

At those conditions particle sizes can be large with no mass transfer restrictions as can be observed in Fig. 4b. Optimal conditions calculated in Table 8 also are in the non-restricted region of Figures 4a and 4b.

In the case of heat transfer, temperature gradients are negligible as Prater numbers shown in Table 8 are near zero, meaning particles are nearly isothermal and maximum temperature difference is lower than 0.1°C. This mean that that the temperature difference between the surface and the center of the particle is negligible.

This is concordant with the results of Abasaeed [38] and Tillman [39] who performed simulations to predict the effect of heat transfer in different particle sizes and showed a very little effect on cellulose and hemicellulose hydrolysis at the conditions tested in this work.

Another important issue is product transport to bulk solution, but available data in literature is not enough to perform estimations. It is important to point that these calculations are mainly overestimations. Real Thiele modulus and Prater numbers should be even lower since porosity would increase as reaction develops due to solubilization of sugar and fragmented polysaccharides; this means effective diffusivity and Thermal conductivity would increase as well. Moreover, particle size would become smaller as the process takes place and the size reduction is more evident in agitated experiments. All those changes during process support the conclusions that the effect of particle size in experimental data shown in Table 5 are not related to intra-particle heat and acid transfer.

4. Discussion

Most studies over particle size rely on the assumption that yield should be lower at higher particle size due to mass and heat gradients within surface and particle center [14,38]. The data obtained in this work indicates that it may not be totally true and that an optimal size can be found. The reason for this effect remains to be explained but we suggest a working hypothesis. Smaller particle size biomass exhibits greater water absorption properties and provoques less available liquid in the liquid phase. Cellulose hydrolysis to oligomers is achieved mostly in the solid phase but oligomer rupture to monomer is in the liquid phase and the oligomer exhibit lower solubility than monomer sugars [40], released oligomers could be recondensed to solid phase and become transformed in a non-sugar derivate [11]. Greater size would allow a bigger amount of free liquid for external hydrolysis to take place and a better conversion yield. In the hydrolysates significant amounts of cellobiose oligomer sugars were found and greater solid load had a negative effect over desirability. However the relationship between liquid absorption and yield to glucose need to be proved experimentally and the relative importance of the hypothesis exposed have to be assessed.

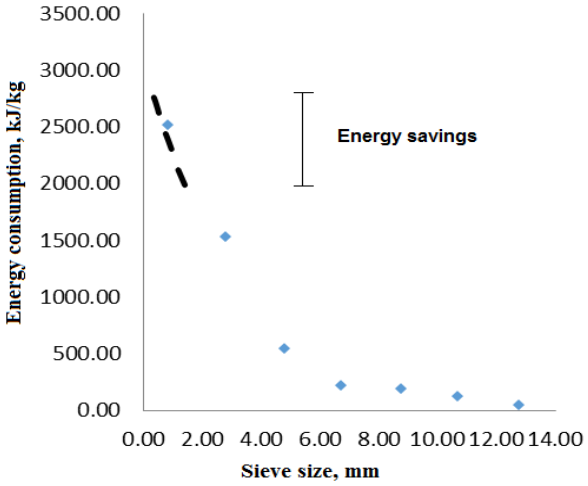

Fig. 5. Energy savings from particle size optimization. Modified from Miao et al., 2011 [41], dashed line is an exponential function adjusted by regression to the data.

Respect to energy consumption for milling, Fig. 5 shows data for milling consumption of wood obtained from Miao et al. [41]. It can be seen that to reach smaller particle size, energy consumption increases exponentially. Our results show that a combination of large particle size and agitation allows a more concentrated solid load and sugar concentrations and yields. The dashed line in Fig. 5 represents energy savings for milling which means that the use of optimal fiber size can save about 892 kJ/kg (278 Wh/kg) which represents about 30% of total energy consumption for wood milling as a pretreatment for ethanol process.

Energy consumption in agitation must be considered. For example, according with data reported by Palmqvist et al., [42] for stirring a suspension of fibers of about 2-10 mm, an L/S of 10 at 600 rpm for about 40 min an energy consumption of 300 kJ/l is needed. Real energy consumption would be less than this since particle size would be reduced as hydrolysis takes place and properties used for calculations in the report are at 35°C. In the real process a high temperature would reduce viscosity and thereby, energy consumption for stirring. It is important to point that this data would be scale-dependent and that optimal stirring rate would change at different impeller geometries.

5. Conclusion

In this work optimal conditions were obtained for wood hydrolysis, particularly particle size shows a very complex effect on process concentrations, yield and selectivity of the reaction. Optimization of particle size allows working with greater solid loads and agitation can be used as a simultaneous saccharification-milling process.

Acknowledgements

We would like to thank the National Council of Science and Technology (CONACYT-Mexico) for the PhD grant and the financial support of this investigation.

References

[1] Holdren JP, Smith KR, Kjellstrom T, Streets D, Wang X, Fischer S. Energy, the environment and health. New York: United Nations Development Programme. 2000;

[2] Galbe M, Zacchi G. A review of the production of ethanol from softwood. Applied microbiology and biotechnology. 2002; 59 (6):618–28.

[3] Drapcho CM, Nhuan NP, Walker TH. Biofuels engineering process technology. McGraw-Hill New York, US; 2008.

[4] Stoeglehner G, Narodoslawsky M. How sustainable are biofuels? Answers and further questions arising from an ecological footprint perspective. Bioresource Technology. 2009; 100(16):3825–30.

[5] Wyman CE. Biomass ethanol: technical progress, opportunities, and commercial challenges. Annual Review of Energy and the Environment. 1999; 24(1):189–226.

[6] Allen SA, Clark W, McCaffery JM, Cai Z, Lanctot A, Slininger PJ, et al. Furfural induces reactive oxygen species accumulation and cellular damage in Saccharomyces cerevisiae. Biotechnol Biofuels. 2010; 3(2):1–10.

[7] LU P, CHEN L, Li G, SHEN S, WANG L, JIANG Q, et al. Influence of furfural concentration on growth and ethanol yield of< i> Saccharomyces kluyveri</i>. Journal of Environmental Sciences. 2007; 19(12):1528–32.

[8] Song S, Lee Y. Acid hydrolysis of wood cellulose under low water condition. Biomass. 1984; 6(1):93–100.

[9] Liu C, Wyman CE. The effect of flow rate of very dilute sulfuric acid on xylan, lignin, and total mass removal from corn stover. Industrial \& engineering chemistry research. 2004; 43(11):2781–8.

[10] Jacobsen SE, Wyman CE. Xylose monomer and oligomer yields for uncatalyzed hydrolysis of sugarcane bagasse hemicellulose at varying solids concentration. Industrial \& engineering chemistry research. 2002; 41(6):1454–61.

[11] Xiang Q, Lee YY, Torget RW. Kinetics of glucose decomposition during dilute-acid hydrolysis of lignocellulosic biomass. Applied biochemistry and biotechnology. 2004; 115(1):1127–38.

[12] Sidiras D, Koukios E. Acid saccharification of ball-milled straw. Biomass. 1989; 19(4):289–306.

[13] Zhao H, Kwak JH, Wang Y, Franz JA, White JM, Holladay JE. Effects of crystallinity on dilute acid hydrolysis of cellulose by cellulose ball-milling study. Energy \& fuels. 2006; 20(2):807–11.

[14] Kim SB, Lee Y. Diffusion of sulfuric acid within lignocellulosic biomass particles and its impact on dilute-acid pretreatment. Bioresource technology. 2002; 83(2):165–71.

[15] Zhu J, Wang G, Pan X, Gleisner R. The status of and key barriers in lignocellulosic ethanol production: A technological perspective. In: Presented as a Keynote Lecture at the International Conference on Biomass Energy Technologies, Guangzhou, China. 2008.

[16] Zhu J, Wang G, Pan X, Gleisner R. Specific surface to evaluate the efficiencies of milling and pretreatment of wood for enzymatic saccharification. Chemical Engineering Science. 2009;64(3):474–85.

[17] Pimenova NV, Hanley TR. Measurement of rheological properties of corn stover suspensions. Applied biochemistry and biotechnology. 2003; 106(1):383–92.

[18] Viamajala S, McMillan JD, Schell DJ, Elander RT. Rheology of corn stover slurries at high solids concentrations-effects of saccharification and particle size. Bioresource technology. 2009;100(2):925–34.

[19] Abràmoff MD, Magalhães PJ, Ram SJ. Image processing with ImageJ. Biophotonics international. 2004; 11(7):36–42.

[20] Fragoso BB, Morales BH, Hernández HV, Cruz MD. Caracterización de la extracción de calor durante el temple de materiales metálicos en un lecho fluidizado con tapón poroso Memorias del XXV Encuentro Nacional AMIDIQ, 2004. CD-ROM (sin número de página).

[21] Martinez A, Rodriguez ME, York SW, Preston JF, Ingram LO. Use of UV absorbance to monitor furans in dilute acid hydrolysates of biomass. Biotechnology progress. 2008; 16(4):637–41.

[22] Derringer G. Simultaneous optimization of several response variables. J. Quality Technol. 1980; 12:214–9.

[23] Bischoff KB. Chemical reactor analysis and design. John Wiley \& Sons Inc; 1990.

[24] Kunihisa K, Ogawa H. Acid hydrolysis of cellulose in a differential scanning calorimeter. Journal of Thermal Analysis and Calorimetry. 1985; 30(1):49–59.

[25] (US) FPL. Wood handbook: wood as an engineering material. United States Government Printing; 1987.

[26] Saeman JF. Kinetics of wood saccharification-hydrolysis of cellulose and decomposition of sugars in dilute acid at high temperature. Industrial \& Engineering Chemistry. 1945; 37(1):43–52.

[27] Thompson DR, Grethlein HE. Design and evaluation of a plug flow reactor for acid hydrolysis of cellulose. Industrial \& Engineering Chemistry Product Research and Development. 1979; 18(3):166–9.

[28] Wu Z, Lee Y. Nonisothermal simultaneous saccharification and fermentation for direct conversion of lignocellulosic biomass to ethanol. In: Biotechnology for Fuels and Chemicals. Springer; 1998. p. 479–92.

[29] Aguilar R, Ram\irez J, Garrote G, Vazquez M. Kinetic study of the acid hydrolysis of sugar cane bagasse. Journal of Food Engineering. 2002; 55(4):309–18.

[30] Jin Q, Zhang H, Yan L, Qu L, Huang H. Kinetic characterization for hemicellulose hydrolysis of corn stover in a dilute acid cycle spray flow-through reactor at moderate conditions. Biomass and Bioenergy. 2011; 35(10):4158–64.

[31] Chen R, Wu Z, Lee Y. Shrinking-bed model for percolation process applied to dilute-acid pretreatment/hydrolysis of cellulosic biomass. Applied biochemistry and biotechnology. 1998; 70(1):37–49.

[32] Sjöström E. Wood chemistry: fundamentals and applications. Academic Pr; 1993.

[33] Ask M, Bettiga M, Mapelli V, Olsson L, others. The influence of HMF and furfural on redox-balance and energy-state of xylose-utilizing Saccharomyces cerevisiae. Biotechnol Biofuels. 2013;6(1):22.

[34] Girisuta B, Janssen L, Heeres H. Kinetic study on the acid-catalyzed hydrolysis of cellulose to levulinic acid. Industrial \& engineering chemistry research. 2007;46(6):1696–708.

[35] Sun Y, Cheng J. Hydrolysis of lignocellulosic materials for ethanol production: a review. Bioresource technology. 2002; 83(1):1–11.

[36] Hamelinck CN, Hooijdonk G van, Faaij AP. Ethanol from lignocellulosic biomass: techno-economic performance in short-, middle-and long-term. Biomass and bioenergy. 2005; 28(4):384–410.

[37] Vidal Jr BC, Dien BS, Ting K, Singh V. Influence of feedstock particle size on lignocellulose conversion—a review. Applied biochemistry and biotechnology. 2011; 164(8):1405–21.

[38] Abasaeed A, Lee Y, Watson J. Effect of transient heat transfer and particle size on acid hydrolysis of hardwood cellulose. Bioresource technology. 1991; 35(1):15–21.

[39] Tillman L, Abaseed A, Lee Y, Torget R. Effect of transient variation of temperature on acid hydrolysis of aspen hemicellulose. Applied Biochemistry and Biotechnology. 1989; 20(1):107–17.

[40] Yang B, Gray MC, Liu C, Lloyd TA, Stuhler SL, Converse AO, et al. Unconventional relationships for hemicellulose hydrolysis and subsequent cellulose digestion. In: ACS symposium series. 2004. p. 100–25.

[41] Miao Z, Grift T, Hansen A, Ting K. Energy requirement for comminution of biomass in relation to particle physical properties. Industrial crops and products. 2011; 33(2):504–13.

[42] Benny P, Magnus W, Gunnar L. Effect of mixing on enzymatic hydrolysis of steam-pretreated spruce: a quantitative analysis of conversion and power consumption. Biotechnology for Biofuels. 2011, 4:10